

# Compressed Sensing Based Dynamic PSD Map Construction in Cognitive Radio Networks

Javad AFSHAR JAHANSHAHI<sup>1,2</sup>, Mohammad ESLAMI<sup>1</sup>, Seyed Ali GHORASHI<sup>1</sup>

<sup>1</sup> Cognitive Telecommunications Research Group, Department of Electrical Engineering, Faculty of Electrical and Computer Engineering, Shahid Beheshti University G.C., Evin 1983963113, Tehran, Iran

<sup>2</sup> Telecommunications and Instrumentation Department, Phase 12, Pars Oil and Gas Company (POGC), National Iranian Oil Company, (NIOC), Iran

j.afshar81@gmail.com, {m\_eslami, a\_ghorashi}@sbu.ac.ir

**Abstract.** *In the context of spectrum sensing in cognitive radio networks, collaborative spectrum sensing has been proposed as a way to overcome multipath and shadowing, and hence increasing the reliability of the sensing. Due to the high amount of information to be transmitted, a dynamic compressive sensing approach is proposed to map the PSD estimate to a sparse domain which is then transmitted to the fusion center. In this regard, CRs send a compressed version of their estimated PSD to the fusion center, whose job is to reconstruct the PSD estimates of the CRs, fuse them, and make a global decision on the availability of the spectrum in space and frequency domains at a given time. The proposed compressive sensing based method considers the dynamic nature of the PSD map, and uses this dynamicity in order to decrease the amount of data needed to be transmitted between CR sensors' and the fusion center. By using the proposed method, an acceptable PSD map for cognitive radio purposes can be achieved by only 20 % of full data transmission between sensors and master node. Also, simulation results show the robustness of the proposed method against the channel variations, diverse compression ratios and processing times in comparison with static methods.*

## Keywords

Power Spectral Density Map (PSD-Map), Cognitive Radio Sensors (CRS), Dynamic Compressive Sensing.

## 1. Introduction

The number of wireless customers as well as their usage of the service will continue to grow, therefore scarce spectrum resources will continue to face huge demands. CR can improve spectrum utilization by allowing secondary users (SUs) to opportunistically access a licensed band provided that the primary user (PU) is absent. To this end, SUs have to sense the spectrum constantly in order to detect the presence of a primary transmitter signal [1]-[3].

Recently, cooperative spectrum sensing algorithms have been proposed to improve the performance of spectrum sensing. PU detection probability can be greatly increased by allowing different SUs to share their information and to create collaboration through distributed transmission/processing, in which each user's information is sent out not only by the user, but also by the collaborating users [4]. Some studies on collaborative spectrum sensing include cooperative scheme design guided by game theory [5], optimum detection-location based method [6], random matrix theory [7], cluster-based cooperative spectrum sensing [8], and distributed rule-regulated cooperative spectrum sensing [9].

In order to enable the CR to reuse the frequency resources and to allow a dynamic spectrum allocation scheme, creating an interference map of the operational region at arbitrary locations and frequencies plays a fundamental rule [10]. When a frequency band is occupied, there could be locations where the transmitted power is low enough so that these frequencies can be reused without suffering from or causing harmful interference to the primary system. These reusable zones may be estimated by means of a collaborative scheme whereby receiving CR Sensors (CRSs) cooperate to estimate the distribution of power in space and frequency as well as localize the positions of transmitting PUs. In [11], sparsity assumption is used in CRs in order to distribute spectrum sensing process and PSD map construction by using Lasso and D-Lasso algorithms. By knowing the spectrum status (i.e. idle or occupied), the remote CRSs can be enabled to reuse dynamically the unoccupied bands. The idea of creating the interference map has been used in [12] in order to build up deterministic power level map with the aim of routing. In addition, in [13] geographical-spectral pattern in CR networks are reconstructed based on the assumption that the pattern is sparse in a certain transform domain.

Compressive sampling is a method for acquisition of sparse signals at rates significantly lower than Nyquist rate, and signal reconstruction is a solution of an optimization problem [14], [15]. In [16], [17], a spectrum sensing scheme based on compressive sampling is introduced which works for special signals whose Fourier transform is

real. In [18], a two-step compressed spectrum sensing scheme for efficient wideband sensing is proposed. In [19], a Bayesian compressive sensing framework reduces the sampling requirements and computational complexity by bypassing signal reconstruction. In [20], to collect spatial diversity against wireless fading, multiple CRs cooperate and establish consensus among local spectral estimate through running a decentralized consensus optimization algorithm. In [21], compressive sampling is performed at local CRs to scan wide spectra, and measurements from multiple CR detectors are fused to collect spatial diversity gain, which improves the detection quality, in particular, under fading channels. Moreover, the authors of [22], [23] have applied matrix completion and joint sparsity recovery to reduce sensing and transmitting requirements and improve sensing results. Specifically, they equipped CR nodes with a frequency selective filter, so the CR nodes sense linear combinations of multiple channel information and report them to the fusion center, where occupied channels are then decoded from the reports by using matrix completion and joint sparsity recovery algorithms. However, in all of these works only a static environment is considered. The authors in [24] proposed a dynamic compressive sensing system in order to detect the occupancy status of a certain channel. They have used the least square technique as a recovery method instead of methods such as  $\ell_1$  minimizations or greedy pursuit algorithms because they believe that this method is the best when the number of changes in PSD status is just one.

Existing papers in the literature mostly focus on the collaborative spectrum sensing performance examination when the master node (fusion center) receives and combines all CR reports. In a  $N$  channel CR network with  $M$  CRs, the master node has to deal with  $N \times M$  reports and combine them wisely in order to form a PSD Map for arbitrary locations in space and frequency domains. However, it is known that wireless channels are subject to fading and shadowing. When SUs experience multi-path fading or happen to be shadowed, the reports transmitted by CR users are subject to transmission loss. As a result in practice, the entire data set of the report is not available at the master node. Besides, when the number of sensors is large, this data transmission which is required for PSD map construction can be challenging. Then, we seek to release CRs from sending, and the master node from gathering such excessively large number of reports, As a consequence, the communication cost, energy consumption and the number of reports sent from the CRs to the master node may significantly be reduced.

The present paper goes in the direction of improving our previous work [25] which gains static compressed sensing in order to construct a dynamic PSD map in frequency, time and space domains, by assuming that the wide-band spectrum has been sensed individually by each CR with one of the mentioned spectrum sensing methods in the literature. Then, the information of changes in spectrum usage at each CR should be transmitted to a master node. To this end, a dynamic compressive sensing based scheme

is presented in order to reduce the amount of this transmitted data. In comparison with a static environment [25], the sensed PSD by each CR is sent to a fusion center, while in dynamic one the recent changes in PSD are transmitted continuously to the fusion center. Therefore, the recent changes of the sensed PSDs at different locations and frequencies is compressed by a certain compression ratio and sent over a Rician fading channel with an AWGN noise to the master node. Master node collects the information from all CRs, reconstructs the received PSDs, constructs the PSD map of each frequency band  $f_i$  and then identifies the available spectrum, accordingly. The identification of the available spectrum is performed by setting a threshold for deciding occupancy of a frequency band based on the comparison between PSD estimates and a minimum power level which is given by the PUs. The recovery process of the received information in the master node is done by taking advantage of compressive sensing methods, e.g. BP [26], OMP [27], Lasso and Lars [28]. The key contribution here is the idea that in order to follow the dynamics of the PSD map, it is only needed to send the changes of the previous status of the PSD map with respect to the new one, with a proper rate. Then, the master node broadcasts the information of PSD maps to all cognitive radios in the support region or directly controls the cognitive radio traffic, itself. Therefore, cognitive radio users in each spatial region are informed of idle parts of the spectrum they can use. Moreover, it should be mentioned that the present work is a comprehensively extended version of our previous one in [31].

The rest of this paper is organized as follows. In Section 2, preliminaries about spectrum sensing problem formulation including topographical PSD map and its benefits, the compressive sampling method, and the compressive sampling based spectrum sensing is introduced. Section 3 contains our proposed method for PSD Map data transmission between CRs and master node in order to build the PSD map. In Section 4, we present the experimental results which show the performance of the proposed method. Finally, the article is concluded in Section 5.

## 2. PSD Map in Space and Frequency

A PSD map is defined in a six dimension  $(x, y, z, t, f, p)$  space, and denotes the usage of the radio resources of time, frequency and power level  $(t, f, p)$ , for any location of  $(x, y, z)$  in the considered geographic area. The necessary dimensions of PSD map to be used in cognitive radio applications including spectrum sensing and opportunistic data transmission in physical layer or medium access control (MAC) layer can be reduced to  $(x, y, r_i)$  where  $r_i \in \{t, f, p\}$ , for the sake of simplicity. This PSD map offers a network-wide knowledge about the quality of different wireless links, thus being significantly helpful for upper layer issues like routing [12] and congestion controls [13] in cognitive radio networks.

In this paper, it is assumed that a sensing approach has been used to get the wide-band spectrum power spectral density by several sensors which are distributed in the considered area. Then, through a master node, CRS cooperate with each other to estimate the distribution of power in space and frequency domains. In this way, the (un)used frequency bands are identified at different locations and times, and thus the spatial frequency reuse is facilitated; the CRSs reuse the idle frequency bands dynamically by knowing the spectrum at any location. PSD map also enables SUs to adapt their transmit-power so as to minimally interfere with PUs. This can be particularly helpful for sensor networks that are supposed to work in an unlicensed frequency band. The decision on the spectrum state (occupied or unoccupied) is made by the comparison of PSD estimations with minimum power levels which have been given by the PUs. The required accuracy of PSD map is determined by the level of accuracy in identification of the (un)used bands, in space, time and frequency domains. In Fig. 1, an exemplary PSD map is shown in three dimensions including frequency band,  $x$  axis and  $y$  axis in a certain time,  $t$ . Fig. 1 helps to better understand how it is possible for the sensor networks to make a connection without causing harmful interference on the PUs.

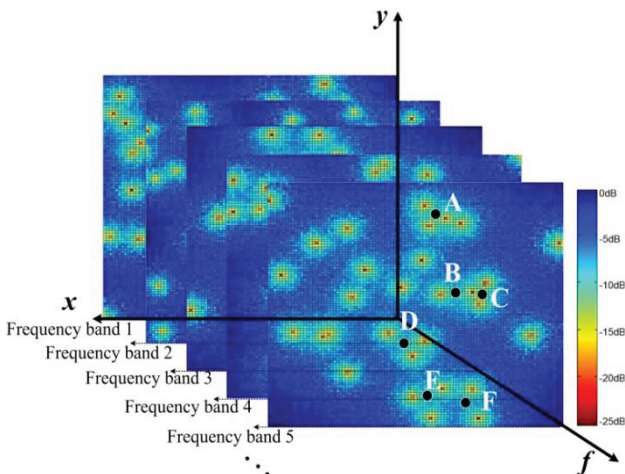


Fig. 1. Illustration of typical PSD maps created by the cooperation of several sensors in distinct frequency bands.

The PSD maps illustrated in Fig. 1 for typical frequency bands have been created by the cooperation of sensor nodes in a zone of support. High energy levels mean that the PUs are active in those areas in the frequency subbands  $f_i, i = \{1, 2, \dots, N\}$ . The PSD map in this figure includes different clusters like A, B, C, D, E and F. The level of energy at the sensed spectrum in clusters A, B, C, D, E and F is low while in other areas the sensed energy level is high. For each frequency band, there is a distinct PSD map. Suppose that there are several CR users and sensors in each cluster. It can be inferred that in order to avoid the interference on the PUs, only the CR users which are placed in the same cluster could connect to each other over the frequency bands  $f_i$ . A given set of points may be

located in a cluster in a certain frequency of  $f_i$  and time  $t_i$ , but not in other frequencies and times.

### 3. Compressive Sensing Based Proposed Model

Wideband spectrum sensing methods try to find the locations of vacant frequency bands (also called spectrum holes), by analyzing the irregularities in the PSD. The basic idea of this approach is to view the entire wide-band spectrum as several subbands, where subband edges indicate changes in spectrum occupancy. These spectrum edges can be detected using different image processing methods such as Mumford shah [29] and wavelet based detectors [30]. The compressive sensing-based spectrum sensing approach works under the assumptions that the PSD is realistic, with relatively flat and almost smooth regions over its supported frequency domain such as the one shown in Fig. 4. The compressive sensing based approach is applied to wide-band spectrum sensing as follows. The transmitted signal from the CRS  $x(t)$  is received and the discrete-time signal stacked into  $P$  size vectors as follows:

$$x_k = [x_{kP} \ x_{kP+1} \ \dots \ x_{kP+P-1}]^T, \quad k = 0, 1, 2, \dots \quad (1)$$

Assuming that the signal is wide-sense stationary with zero mean, the autocorrelation vector can be found as a vector with size  $N$ :

$$r_x^k = [0 \ r_x(-N+1) \ \dots \ r_x(0) \ \dots \ r_x(N-1)]^T \quad (2)$$

where  $N = 2P$ . A smoothing operator  $\mathbf{W}$  followed by Fourier transform  $F$  are then performed to  $r_x^k$  as  $S_x^k = \mathbf{F}\mathbf{W}r_x^k$  where the size of  $\mathbf{W}$  and  $\mathbf{F}$  matrices are  $N \times N$ . Assuming that the PSD is almost flat and piecewise constant, the edge map of the vector  $S_x^k$  will be sparse. This edge map can easily be found by using difference operator (first derivation) or second derivation of the vector. This means that, the number of significant singularities in the PSD,  $S_x^k$ , and consequently the number of significant non-zero values in the difference vector,  $Z_s^k$  are much smaller than  $N$ . The edge map operator can be performed by using

$$Z_s^k = \mathbf{\Gamma} (S_x^k - S_x^{k-1}) \quad (3)$$

where

$$\mathbf{\Gamma} = \begin{bmatrix} 1 & 0 & \dots & 0 \\ -1 & 1 & \dots & 0 \\ 0 & \ddots & \ddots & \vdots \\ 0 & \dots & -1 & 1 \end{bmatrix} \quad (4)$$

or

$$Z_s^k = \mathbf{\Gamma} \mathbf{F} \mathbf{W} (r_x^k - r_x^{k-1}) = \mathbf{G}^{-1} (r_x^k - r_x^{k-1}). \quad (5)$$

Now we can use the compressive sensing theorem in order to take  $K$  samples from vector  $r_x^k$  by using a  $K \times N$  measurement matrix  $\mathbf{\Phi}$  as

$$C_x^k = \mathbf{\Phi} (r_x^k - r_x^{k-1}) \quad (6)$$

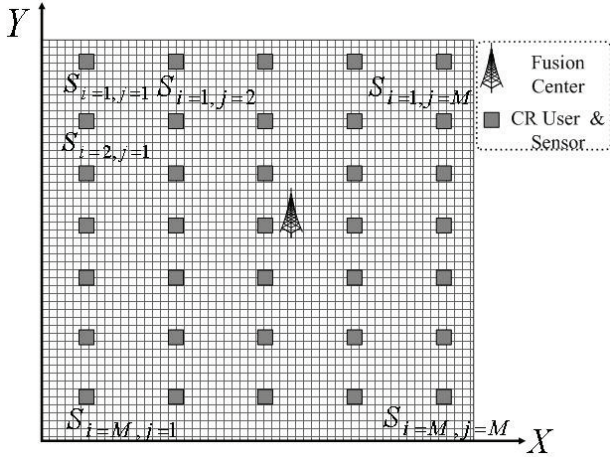


Fig. 2. A typical scenario of CRSs, user and master node in the considered area.

Thus, in the reconstruction process, the sparse edge map vector can be found from  $C_x^k$  by solving the following optimization problem:

$$\tilde{Z}_s^k = \arg \min_{Z_s^k} \|\tilde{Z}_s^k\|_1 \quad (7)$$

subject to  $C_x^k = (\Phi G)Z_x^k$

and the estimated PSD will be achieved as:

$$\hat{S}_x^k(n) = \sum_{i=1}^n (\tilde{Z}_s^k(i) + \tilde{Z}_s^{k-1}(i)), \quad n = 1, 2, \dots, N. \quad (8)$$

#### 4. Proposed Method for Dynamic PSD Map Data Transmission between CRSs and Master Node

Since the dynamic PSD map problem is divided into a sequence of time periods, in a dynamic environment,  $S_x^k$  changes continuously. In this paper we assume that PSD map experiences changes due to the PUs way of spectrum usage, for example a certain PU starts or stops using a frequency band, or changes the level of the sending power in one channel, significantly.

In order to explain the proposed algorithm for PSD map construction, consider the following scenario. Suppose that the CRS are distributed in the observed scenario as shown in Fig. 2. The first step is to sense PSD in each CRS, ( $S_x^{i,j,k-1}$ ) and send it to the master node. Sensing PSDs can be performed by one of the mentioned schemes described in Section 1. These sensed PSDs are saved in a buffer at CRSs for a certain time, instead of sending the amount of  $S_x^{i,j,k}$  to the master node, the amount of  $\Delta S_x^{i,j,k} = S_x^{i,j,k} - S_x^{i,j,k-1}$ , which means the changes in the sensed PSD, is sent to the master node for the period time  $k^{th}$ . So, the attained  $K$ - dimensional  $c_x^{i,j,k}$ ,  $i = \{1, 2, \dots, M\}, j = \{1, 2, \dots, M\}$  vector (6) from the  $(i, j)^{th}$  CRS is sent to the master node. The channel parameters among the sensors and master node depend on the distance, noise levels, geographical tomography, etc.

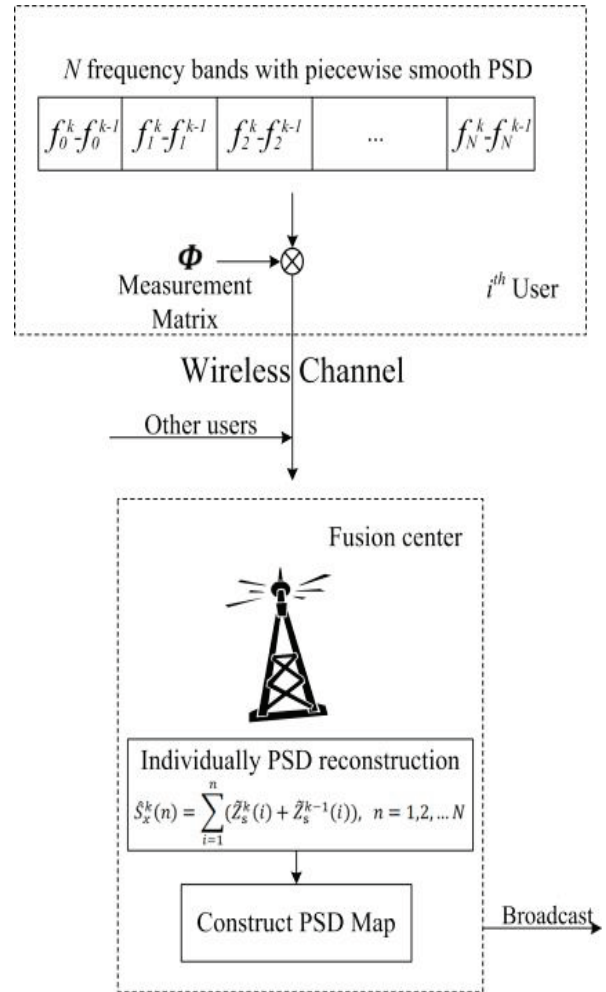


Fig. 3. PSD Map creation by individually PSD reconstruction of all CRSs [31].

In the master node, in order to reconstruct each observed PSD, the base station solves (7) for each received  $c_r^{i,j,k}$  and finds the  $\tilde{Z}_r^{i,j,k}$ . Consequently, the reconstructed PSD ( $\hat{S}_r^{i,j,k}$ ) can be obtained by using (8) and the achieved  $\tilde{Z}_r^{i,j,k}$ . The master node collects these  $\hat{S}_r^{i,j,k}$ 's that come from each sensor and can construct the spatial-frequency PSD map by interpolating. The proposed algorithm for PSD map construction is depicted in Fig. 3. The overall proposed algorithm is as follows:

**Step 1:** Each sensor located in the  $(i, j)^{th}$  grid point where  $i = \{1, 2, \dots, M\}, j = \{1, 2, \dots, M\}$ , senses the PSD of the channel in its local region in time  $k$  and calculates its difference to the previous sample at time  $k - 1$ ,  $\Delta S_x^{i,j,k}$ . Then, each achieved  $c_x^{i,j,k}$  (6) will be sent to the master node.

**Step 2:** For each received  $c_r^{i,j,k}$ , the master node solves (7) and finds the corresponding  $\tilde{Z}_r^{i,j,k}$ .

**Step 3:** For each calculated  $\tilde{Z}_r^{i,j,k}$ , the master node solves (8) to estimate the related PSD in time  $k$ ,  $\hat{S}_r^{i,j,k}$ .

**Step 4:** Master node collects all the reconstructed

$\hat{S}_r^{i,j,k}$ ,  $i = \{1, 2, \dots, M\}, j = \{1, 2, \dots, M\}$ . By considering the location of each grid node (the location of each CRS  $(i, j)$ ), master node fits a 2-D interpolation such as bilinear method in order to construct the PSD map in each frequency subband,  $f_i$ .

## 5. Simulation Results and Discussion

In this section, the evaluation of the proposed method of PSD map data transmission in different experimental scenarios is considered. In simulation results we individually reconstruct PSDs in order to create PSD maps using Procedure 1.

<b>Procedure 1.</b> Procedure of reconstruction PSDs in order to construct PSD maps.	
1:	Uniformly distribute $M \times M$ CR sensors in the region of support.
2:	<b>for</b> time= $t$ : number of time periods <b>do</b>
3:	<b>for</b> $i=1$ :number of CR sensors <b>do</b>
4:	Sense wide-band spectrum in time $t$ .
5:	Compute the difference between sensed PSD in time $t$ and $t - 1$ .
6:	Compute the edges and multiply by measurement matrix $\Phi$ in a certain compression ratio $K/N$ . Then send over the channel.
7:	Generate the path-gains and path-delays of the channel fading.
8:	Compute the received information and reconstruct individually the PSD of the CRS $i^{\text{th}}$ .
9:	<b>end for</b>
10:	Construct the PSD maps in time $t$ by using reconstructed PSDs of all CR sensors.
11:	<b>end for</b>
12:	Output all PSD maps.

**Tab. 1.** Procedure of PSDs reconstruction in the fusion center.

In order to simulate the PSD map, the following constrains are considered:

- The PSD of each sensor consists of 32 frequency subbands while each channel interval contains 8 samples (therefore,  $N = 256$ ). Fig. 4 shows a typical PSD which is related to the sensor  $i = 1, j = 1$ .

- Occupancy and un-occupancy of each subband is modeled as a random number.

- While the occupancy state of the subbands is modeled as a random number, we assume that neighbor sensors should sense similar energy levels in frequency subbands. Fig. 5 depicts a 3D representation of a PSD map in a fixed frequency in which, regions with higher and lower values show occupied and unoccupied spatial zones in that frequency, respectively.

- The sensing zone consists of  $M \times M$  ( $M = 34$ ) uniformly distributed sensors.

As we have considered a wireless sensor network scenario for CRSs in an open area, all of the experimental results are simulated by using a Rician channel with 3 paths by different path-gains and delays depending on the relative locations of the sensors with respect to the master node. The spatial distribution of Rician channel's path gains (dB) and the normalized Rician channel's path delay

for each CRS are depicted in Fig. 6, respectively. The maximum of each path-gains are  $[10e-1; 9.0e-01; 8.0e-1]$  (dB), the minimum of each path delays are  $[1.0000e-015; 1.0000e-017; 1.0000e-019]$  seconds.

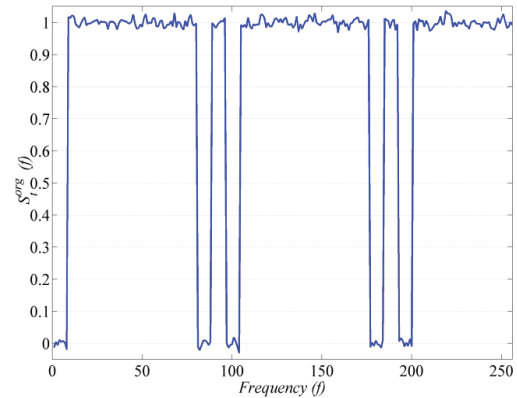


**Fig. 4.** An example of a sensed PSD by a sensor  $(i, j = 1)$ .

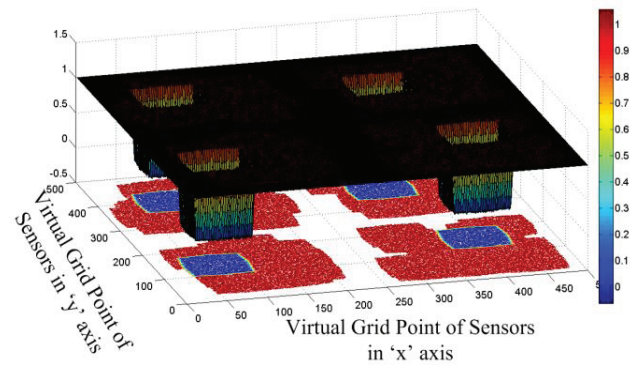


**Fig. 5.** A 3D representation of a PSD Map in a given frequency subband.

It is clearly shown that when one CRS is far away from the master node, the received signal is very weak, therefore the farthest CRS' data over the channel experiences the maximum delay and minimum path-gain and vice versa. In addition, we assume an additive white Gaussian noise with different noise levels. Measurement matrix  $\Phi$  for all of the sensors is identical and designed by Discrete Cosine Transform (DCT) dictionary. This section consists of five different simulation sets which are explained as follows.

### 5.1 SNRs of $C_x^k$

Our simulations were done with different SNRs of  $C_x^k$ . In this subsection, we discuss several factors that determine the SNR of  $C_x^k$ : the SNR of  $\Phi r_x^{k-1}$  and  $\Phi r_x^k$ , as well as the powers of the changed channel. The SNR of  $\Phi r_x^{k-1}$  further depends on the level of thermal noise, the accuracy of the recovered  $r_x^{k-1}$  (since some entries of  $\Phi r_x^{k-1}$  are not directly received but recovered from  $\Phi r_x^{k-1}$ ), as well as the length of the previous time period, during which there is no significant change in the channel powers. The SNR of  $\Phi r_x^{k-1}$  usually improves over time as more measurements are received and noise gets averaged

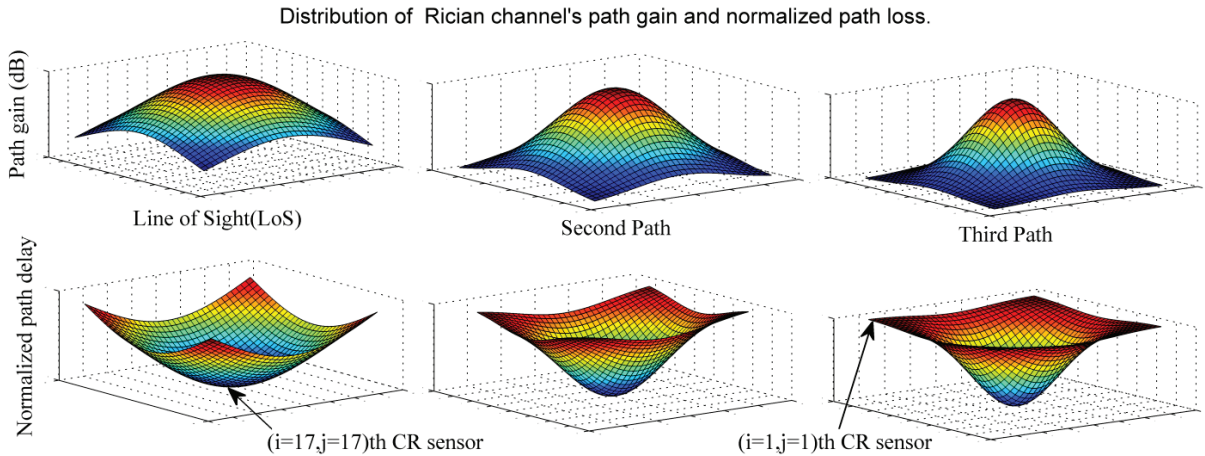


Fig. 6. Spatial distribution of Rician channel's path gains (dB) and normalized path delay: Line of Sight, second and third path, respectively.

over time. Hence, the longer the stationary period, the higher the SNR. The SNR of  $\Phi r_x^k$  also depends on the thermal noise level and the number of measurements received.

However, the missing entries of  $\Phi r_x^k$  are not used. For fixed SNRs of  $\Phi r_x^{k-1}$  and  $\Phi r_x^k$ , the SNR of  $C_x^k$  will be higher if the change in power (i.e., the signal of  $C_x^k$ ) is stronger, which translates to the unique nonzero rows of  $(r_x^k - r_x^{k-1})$  containing larger values. Physically, if a nearby or high-power PR starts or stops, the SNR of  $C_x^k$  will be large. On the contrary, if a distant or low-power PR starts or stops, the SNR of  $C_x^k$  will be small. Since the SNR of  $C_x^k$  depends on several factors, it is tedious to run simulations with all the factors varying. Instead, we directly varied the SNRs of  $C_x^k$ .

### 5.2 Average Unsuccessful Detection Rate vs. Compression Ratio (K/N)

In Fig. 7, we show average fail rate versus the sampling rate, which is defined as the number of received entries of  $C_x^k$  over its total number of entries. We varied the sampling rate from 5 % to 40 %. Note that  $C_x^k$  is already highly compressed as compressive sensing is applied to  $r_x$ , and the reference of our sampling rate is to the size of  $C_x^k$ , not that of  $r_x$ . Figures 5(a) and (b) correspond to the performance for SNR = 10 dB and SNR = 20 dB, respectively. When SNR = 10 dB (shown in Fig. 7a), we only need less than 25 % of the samples at the fusion center to guarantee a successful detection. As SNR increased to 20 dB (shown in Fig. 7 b), the sampling rate can be further reduced to 20 % for reliable detection.

### 5.3 Reconstructed PSD

This simulation shows the capability of the proposed method in reconstruction of the sensed PSDs in master node. The considered PSD is the  $S_x^{1,1}$  which is sampled by

compressive sensing method by a compression rate of  $K/N = 20 \%$ , and then, the corresponding  $c_x^{1,1,k}$  is sent over a 3 path Rician channel with 20 dB SNR value.

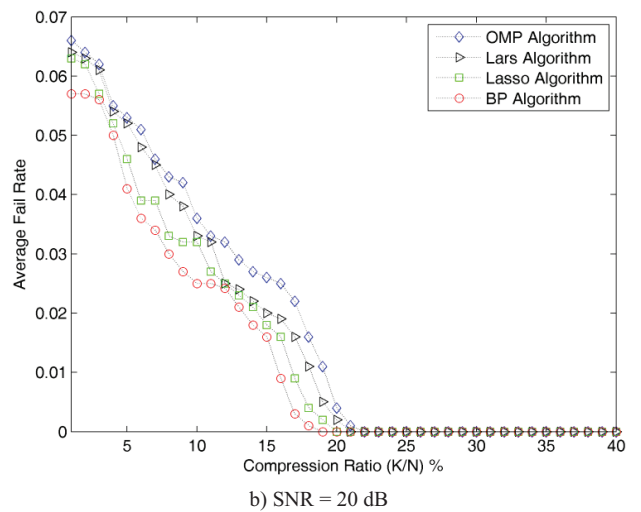
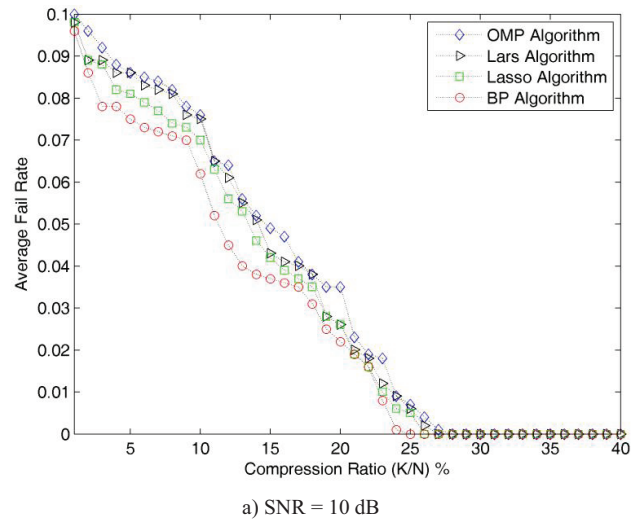


Fig. 7. Average rate (300 runs each point) of correct recovery.

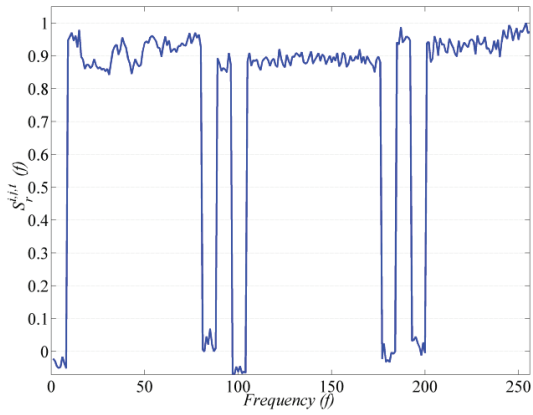


Fig. 8a. Reconstructed PSD by BP method.

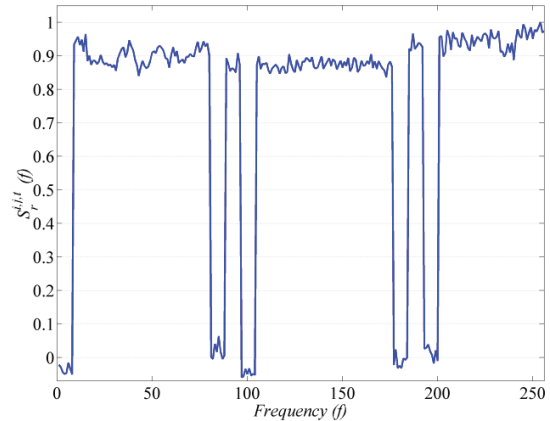


Fig. 8c. Reconstructed PSD by OMP method.

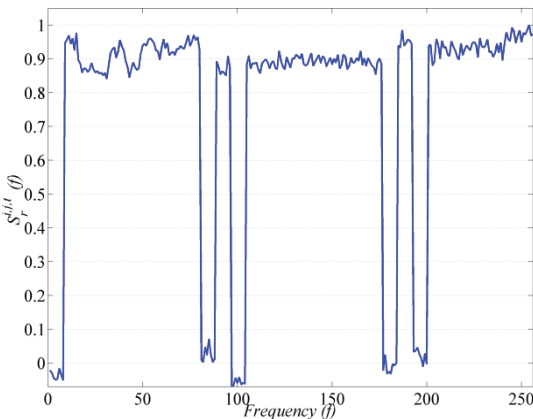


Fig. 8b. Reconstructed PSD by Lasso method.

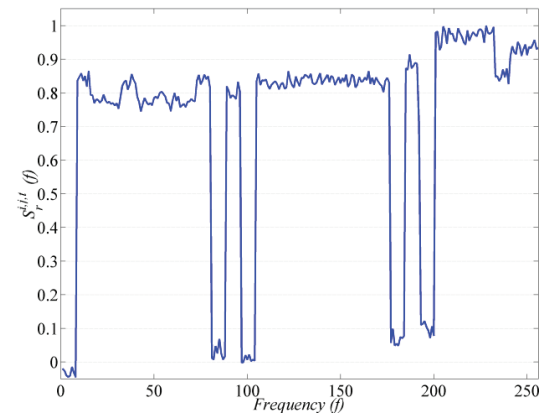


Fig. 8d. Reconstructed PSD by Lars method.

In order to solve (7), the solvers BP, OMP, Lars and Lasso have been used and their reconstructed PSDs are shown in Fig. 8. It can be inferred that the reconstructed PSD by BP, Lasso and OMP are closer to the transmitted one which is shown in Fig. 4, particularly in the place of the PSD edges and its reconstructed values. But in the reconstructed PSD by OMP and Lars, some mistakes in the calculation of the magnitude of the reconstructed PSD are happened in some frequency bands. It is because of the channel variations and path delays.

### 5.4 RMS Error Performances

We compute the normalized RMSE between the referenced and the estimated PSDs, which is defined as

$$RMSE = \frac{\sum_{m=1}^{M^2} \sqrt{\sum_{n=1}^N |f_{n,m} - \hat{f}_{n,m}|^2}}{N.M^2} \quad (9)$$

where  $f_{n,m}$  denotes the  $n^{th}$  PSD sample of the  $m^{th}$  CR sensor which has been sent to the master node and  $\hat{f}_{n,m}$  is the  $n^{th}$  sample of the estimated PSD in the master node related to the  $m^{th}$  sensor data.  $N$  is the number of PSD samples and  $M^2$  is the number of all CR sensors which has

been placed in the region of support. The RMS error performance is considered with respect to several different SNRs as well as different compression ratios  $K/N$  in both static [25] and dynamic models. Fig. 9 shows the comparison of the RMS error performance of the BP, Lasso, OMP and Lars methods in both static [25] and dynamic models in SNR = 5 dB and 25 dB. As we expected, the RMS error of the dynamic algorithm is lower than the static one. The dynamic model is not only simpler but also outperforms the static one. Since each period requires solutions from its previous period, the success of dynamic recovery is based on the success in every period. On the other hand, in case dynamic model fails due to either lack of measurement or inaccurate previous solution, the model should be changed to standard one and the PSD at each CRS must be send completely.

Moreover, the performance of reconstruction will be improved for all four approaches when the compression ratio  $K/N$  grows up. While the RMSE performance of the Lars method is worse than others, BP and Lasso methods have got better performance compared to the other two. Also, by increasing the compression ratio  $K/N$ , the RMSE performance of the methods merges to each other.

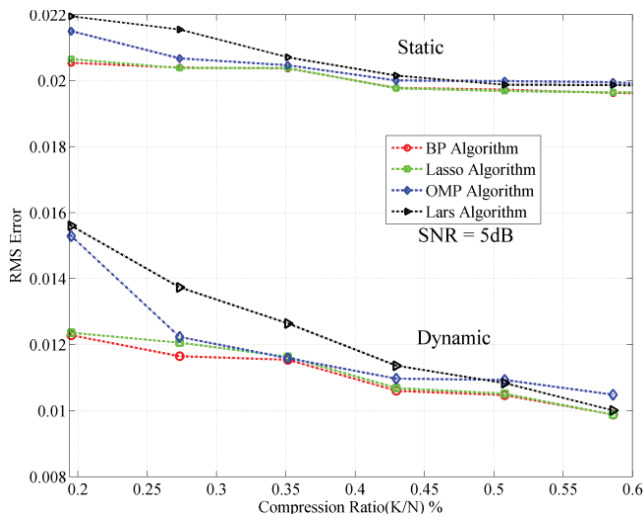


Fig. 9a. Comparison of the RMS Error performance of the BP, Lasso, OMP and Lars methods in both static [25] and dynamic models in SNR = 5 dB.

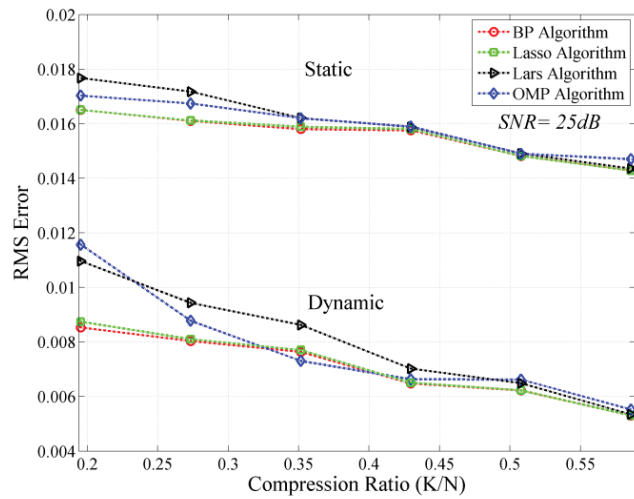


Fig. 9b. Comparison of the RMS Error performance of the BP, Lasso, OMP and Lars methods in both static [25] and dynamic models in SNR = 25 dB.

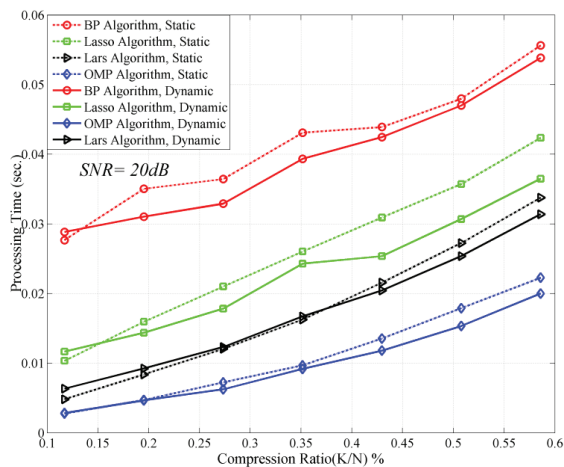


Fig. 10. Reconstruction PT versus compression ratio K/N in SNR = 20 dB for both static [25] and dynamic algorithms.

### 5.5 Process Time

In order to evaluate how quickly the master node can solve the reconstruction in (7) and (8), the Process Time (PT) is defined as follows:

$$PT = \frac{\sum_{m=1}^{M^2} t_{m,K}}{M^2} \tag{10}$$

where  $t_{m,K}$  is the reconstruction time of the  $m^{th}$  CR sensor PSD in a distinct comparison rate  $K$ . It is clear that by increasing the  $K/N$  ratio, the  $PT$  grows up as it is shown in Fig. 10. Since the dynamic model requires fewer measurements than the static one, the reconstruction times of the dynamic model decreased. In addition, as mentioned before, while the BP and Lasso methods have got better performance than the other two, their processing time is worse than OMP and Lars methods. These results are attained by a system with Matlab 2009, Processor Intel(R) Core(TM) i7 2.67 GHz, RAM 6.00 GB and 64-bit operating system.

### 5.6 ROC Comparisons

The receiver operating characteristic (ROC) curve is an established means to evaluate the spectrum sensing system performance. These ROC curves plot the probability of *miss-detection* ( $P_m$ ), the probability that the CR fails to detect the presence of the PU, versus the probability of *false-alarm* ( $P_f$ ), the probability that the CR decides the PU is in operation while it was actually off. Missed detection and false-alarm probabilities are defined as follows:

$$P_m = P(\mathcal{H}_0^{CN} | \mathcal{H}_1^{PN}), \tag{11}$$

$$P_f = P(\mathcal{H}_1^{CN} | \mathcal{H}_0^{PN}) \tag{12}$$

where  $\mathcal{H}_i^{PN}$  denotes the actual absence (for  $i = 0$ ) and the actual presence (for  $i = 1$ ) of the primary signal respectively,  $\mathcal{H}_i^{CN}$  indicates the decision made based on the received signals during the spectrum sensing process at the cognitive terminal on the absence (for  $i = 0$ ) and on the presence (for  $i = 1$ ) of the primary transmitter signal. Fig. 11 shows the ROC curves for BP, OMP, Lasso and Lars algorithms in SNR = 10 dB in both static [25] and dynamic models. It is clearly seen that the low RMS error values cause low false alarms and missed detections in the dynamic model. In order to show the sensitivity to the choice of the  $K/N$  values, Fig. 12 depicts the ROC curves for BP, Lasso Lars and OMP algorithms in dynamic model for SNR=30dB for  $K/N= 20\%$  and  $97\%$ , respectively. The distinguished areas have zoomed out to clarify the performance of the algorithms. It is observed that, by increasing the comparison ratio of  $K/N$ , the performance of the four compressive sensing methods become more similar to each other.

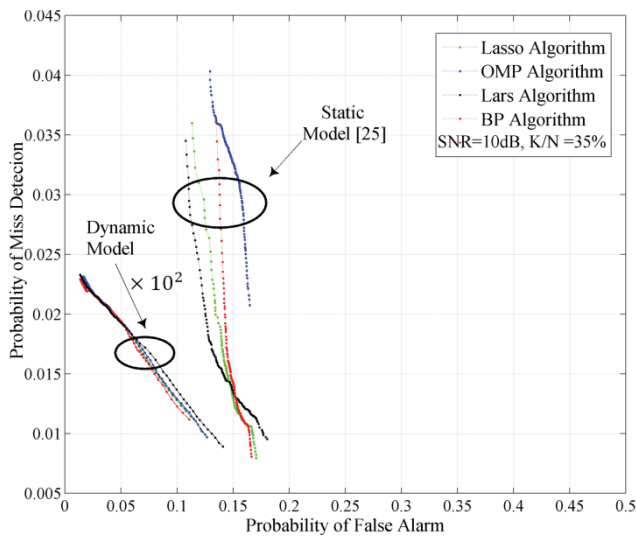


Fig. 11. ROC curves obtained by BP, Lasso, Lars and OMP algorithms in SNR = 10 dB for both static [25] and dynamic schemes.

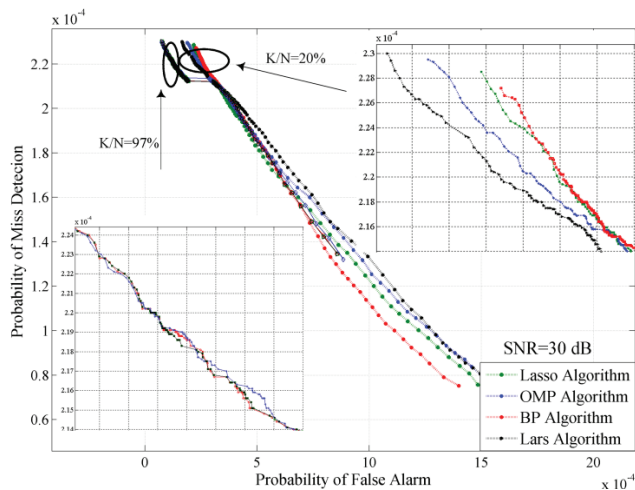


Fig. 12. ROC curves obtained by BP, Lasso, Lars and OMP algorithm for SNR = 30 dB in K/N = 20 % and 97 % respectively.

## 6. Conclusion

Compressive sampling is a method for acquisition of sparse signals at rates significantly lower than Nyquist rate, and this idea has been used in this paper for cognitive radios. In this paper, in order to transmit the CR sensors' data to the master node at a sampling rate lower than the Nyquist rate, a dynamic compressive sensing based scheme is presented. Instead of sending the whole PSD, just the changes between the current PSD status and previous one is sent to the master node. While static (standard) compressive sampling algorithms have to reconstruct received PSD of each sensor, a dynamic algorithm needs to reconstruct the recent changes, which is either a released frequency band or an occupied one of each sensor's PSD. On the other hand, the dynamic compressed sensing algorithm reconstructs the changes just in time. We have shown that the proposed dynamic based algorithm outperforms the

static (standard) model in several simulated conditions. The capability of the proposed method in PSD map construction and its benefits are shown in this paper by simulation results and comparison between the standard and dynamic models are comprehensively discussed. Moreover, it is shown that using the compressive sensing based methods such as BP, Lasso, OMP and Lars increases the performance level of the reconstructed PSDs and decreases the interferences on primary users.

## Acknowledgements

The authors would like to acknowledge the Cognitive Telecommunications Research Group, Faculty of Electrical and Computer Engineering, Shahid Beheshti University G.C. for supporting this work under grant number 600/2183. Moreover, the author Javad Afshar Jahanshahi would like to thank the Pars Oil and Gas Company (POGC) as a wholly owned subsidiary of National Iranian Oil Company (NIOC) for their support and grateful help.

## References

- [1] LONG, J., ZHANG, X., WU, Q. State transition probability based sensing duration optimization algorithm in cognitive radio. *IEICE Transaction on Communications*, 2010, vol. E93-B, no. 12, p. 2099 - 2106.
- [2] TAFAGHODI KHAJAVI, N., SADEGHI IVRIGH, S., SADOUGH, S. M. S. A novel framework for spectrum sensing in cognitive radio networks. *IEICE Transactions on Communications*, 2011, vol. E94-B, no. 9, p. 2600 - 2609.
- [3] TAFAGHODI KHAJAVI, N., SADEGHI IVRIGH, S., SADOUGH, S. M. S. Achievable outage rates in cognitive radio networks under imperfect spectrum sensing. *Radioengineering*, 2012, vol. 21, no. 2, p. 683 - 693.
- [4] YUCEK, T., ARSLAN, H. A survey of spectrum sensing algorithms for cognitive radio applications. *IEEE Communications Surveys and Tutorials*, 2009, vol. 11, no. 1, p. 567 - 575.
- [5] SAAD, W., HAN, Z., DEBBAH, M., HJØRUNGNES, A., BASAR, T. Coalitional games for distributed collaborative spectrum sensing in cognitive radio networks. In *Proceedings of the IEEE Conference on Computer Communications*. Rio de Janeiro (Brazil), 2009, p. 176 - 181.
- [6] ZHANG, H., WANG, X., KUO, G., BOHNERT, T. M. Optimum detection location-based cooperative spectrum sensing in cognitive radio. *Radioengineering*, 2010, vol. 19, no. 4, p. 552 - 560.
- [7] CARDOSO, L. S., DEBBAH, M., BIANCHI, P., NAJIM, J. Cooperative spectrum sensing using random matrix theory. In *Proceedings of the International Symposium on Wireless Pervasive Computing*. Santorini (Greece), 2008, p. 234 - 239.
- [8] SUN, C., ZHANG, W., LETAIEF, K. B. Cluster-based cooperative spectrum sensing in cognitive radio systems. In *Proceedings of the IEEE International Conference on Communications*. Glasgow (Scotland), 2007, p. 254 - 259.
- [9] CAO, L., ZHENG, H. Distributed rule-regulated spectrum sharing. *IEEE Journal on Selected Areas in Communications: Special Issue on Cognitive Radio: Theory and Applications*, 2008, vol. 26, no. 1, p. 130 - 145.
- [10] ZHAO, Q., SADLER, B. A survey of dynamic spectrum access. *IEEE Signal Processing Magazine*, 2007, vol. 24, no. 3, p. 79 - 89.

- [11] BAZERQUE, J. A., GIANNAKIS, G. B. Distributed spectrum sensing for cognitive radio networks by exploiting sparsity. *IEEE Transactions on Signal Processing*, 2010, vol. 58, no. 3, p. 1376 - 1387.
- [12] LI, H. Reconstructing geographical-spectral pattern in cognitive radio networks. In *Proceedings of the IEEE 5<sup>th</sup> International Conference on Cognitive Radio Oriented Wireless Networks & Communications (CrownCom)*. Cannes (France), 2010, p. 1 - 5.
- [13] SHIH, S. Y., CHEN, K. C. Compressed sensing construction of spectrum map for routing in cognitive radio networks. In *Proceedings of the IEEE 73<sup>rd</sup> VTC*. Budapest (Hungary), 2011, p. 1 - 5.
- [14] CANDES, E., ROMBERG, J., TAO, T. Robust uncertainty principles: Exact signal reconstruction from highly incomplete frequency information. *IEEE Transactions on Information Theory*, 2006, vol. 52, no. 2, p. 489 - 509.
- [15] DONOHO, D. L. Compressed sensing. *IEEE Transactions on Information Theory*, 2006, vol. 52, no. 4, p. 1289 - 1306.
- [16] TIAN, Z., GIANNAKIS, G. B. Compressed sensing for wide-band cognitive radios. In *Proceedings of the International Conference on Acoustics, Speech, and Signal Processing*. Honolulu (USA), 2007, p. IV/1357 - IV/1360.
- [17] POLO, Y. L., WANG, Y., PANDHARIPANDE, A., LEUS, G. Compressive wide-band spectrum sensing. In *Proceedings of the International Conference on Acoustics, Speech, and Signal Processing*. Taipei (Taiwan), 2009, p. 1 - 4.
- [18] WANG, Y., TIAN, Z., FENG, C. A two-step compressed spectrum sensing scheme for wideband cognitive radios. In *Proceedings of IEEE Global Telecommunications Conference*. Florida (USA), 2010, p. 1 - 5.
- [19] HONG, S. Multi-resolution Bayesian compressive sensing for cognitive radio primary user detection. In *Proceeding of IEEE Global Telecommunications Conference*. Florida (USA), 2010, p. 37 - 42.
- [20] ZENG, F., LI, C., TIAN, Z. Distributed compressive spectrum sensing in cooperative multi-hop cognitive networks. *IEEE Journal of Selected Topics in Signal Processing*, 2011, vol. 5, no. 1, p. 37 - 48.
- [21] TIAN, Z., BLASCH, E., LI, W., CHEN, G., LI, X. Performance evaluation of distributed compressed wideband sensing for cognitive radio networks. In *Proceeding of 11<sup>th</sup> International Conference on Information Fusion*. Cologne (Germany), 2008, p. 1 - 5.
- [22] MENG, J., YIN, W., LI, H. HOSSAIN, E., HAN, Z. Collaborative spectrum sensing from sparse observations in cognitive radio networks. *IEEE Journal of Selected Areas in Communications*, 2011, vol. 29, no. 2, p. 327 - 337.
- [23] MENG, J., YIN, W., LI, H. HOSSAIN, E., HAN, Z. Collaborative spectrum sensing from sparse observations using matrix completion for cognitive radio networks. In *Proceedings of the International Conference on Acoustics, Speech, and Signal Processing*. Florida (USA), 2010, p. 3114 - 3117.
- [24] YIN, W., WEN, Z., LI, S., MENG, J., HAN, Z. Dynamic compressive spectrum sensing for cognitive radio networks. In *Proceeding of 45<sup>th</sup> Annual Conference on Information Sciences and Systems (CISS)*. Baltimore (USA), 2011, p. 1 - 6.
- [25] AFSHAR JAHANSHAHI, J., ESLAMI, M., GHORASHI, S. A. PSD map construction scheme based on compressive sensing in cognitive radio networks. *IEICE Transactions on Communications (Special Issue on Cognitive Radio Networks)*, 2012, vol. E95-B, no. 4, p. 1056 - 1065.
- [26] LA, C., DO, M. N. Signal reconstruction using sparse tree representation. In *Proceedings of the SPIE Conference on Wavelet Applications in Signal and Image Processing*. San Diego (USA), 2005, p. 1 - 5.
- [27] DONOHO, D. L., ELAD, M., TEMLYAKOV, V. Stable recovery of sparse over complete representations in the presence of noise. *IEEE Transactions on Information Theory*, 2006, vol. 52, no. 1, p. 6 - 18.
- [28] TIBSHIRANI, R. Regression shrinkage and selection via the Lasso. *Journal of Royal Statistics Society, Series B*, 1996, vol. 58, no. 1, p. 267 - 288.
- [29] ESLAMI, M., SADOUGH, S. M. S. Wideband spectrum sensing for cognitive radio via Phase-Field segmentation. In *Proceedings of the Conference on Wireless Advanced*. London (UK), 2010, p. 1 - 4.
- [30] TIAN, Z., GIANNAKIS, G. B. A wavelet approach to wideband spectrum sensing for cognitive radios. In *Proceeding of International Conference on Cognitive Radio Oriented Wireless Networks and Communications*. Florida (USA), 2006, p. 1 - 4.
- [31] AFSHAR JAHANSHAHI, J., ESLAMI, M., GHORASHI, S. A. Dynamic PSD map construction based on compressed sensing in cognitive radio networks. In *Proceeding of IEEE International Symposium on Telecommunications (IST)*. Tehran (IRAN), 2012, p. 363 - 366.

## About Authors ...

**Javad AFSHAR JAHANSHAHI** received his B.Sc. and M.Sc. Degrees both in Electrical Engineering from the University of the Sistan & Baluchestan and Shahid Beheshti University, in 2006 and 2010, respectively. Now he is a member of Telecommunications and Instrumentation Department, Pars Oil and Gas Company (POGC), National Iranian Oil Company (NIOC) and Cognitive Telecommunications Research Group, Department of Electrical Engineering, Shahid Beheshti University G.C., in Tehran, Iran. His research interests are in wireless cognitive radio, and wireless communications.

**Mohammad ESLAMI** is currently pursuing PhD. program in Communication Engineering in Shahid Beheshti University G.C., Tehran, Iran. He is a member of Cognitive Telecommunication Research Group, Department of Electrical Engineering, Shahid Beheshti University G.C. His focus is on mathematical image and video processing, stereo and multi view vision systems. His research interests includes: mathematical image & video processing, cognitive radio & spectrum sensing, stereo & multi-view vision.

**Seyed Ali GHORASHI** received his B.Sc. and M.Sc. degrees in Electrical Engineering from the University of Tehran, Iran, in 1992 and 1995, respectively. Then, he joined SANA Pro Inc., where he worked on modeling and simulation of OFDM based wireless LAN systems and interference cancellation methods in W-CDMA systems. Since 2000, he worked as a research associate at King's College London on "capacity enhancement methods in multi-layer W-CDMA systems" sponsored by Mobile VCE. In 2003, He received his PhD at King's College and since then he worked at Kings College as a research fellow. In 2006 he joined Samsung Electronics (UK) Ltd as a senior researcher and now he is a faculty member of Cognitive Telecommunication Research Group, Department of Electrical Engineering, Shahid Beheshti University G.C., in Tehran, Iran, working on wireless communications.